Best Practices in Physics-based Fault Rupture Models for Seismic Hazard Assessment of Nuclear Installations: issues and challenges towards full Seismic Risk Analysis. Cadarache-Chateau, France, 14-16 May 2018

GUTENBERG-RICHTER'S B-VALUE AND EARTHQUAKE ASPERITY MODELS

P. SENATORSKI

Institute of Geophysics, Polish Academy of Sciences, Warsaw, Poland.

E-mail contact: psenat@igf.edu.pl

Abstract. The Gutenberg-Richter (G-R) relationship can be derived as the Gibbs distribution. For a given earthquake set (all earthquakes in a given region, time period, magnitude range, tectonic settings) the Gibbs probability density function for magnitudes, with a given b-value in its exponent, is the most uniform distribution under the constraints of the magnitude range and mean value. Therefore, it represents our limited knowledge about the system output: The only piece of information is the mean value. Honest earthquake forecasts can be based on such a distribution, since it represents all and only available information about the seismic system. The b-value can change among different earthquake sets (in time, space, magnitude ranges, or tectonic settings), since it is related to earthquake rupture dynamics, or seismic source characteristics. The relationship between the b-value and the exponent β in the rupture area vs. maximum slip scaling, $A \propto D^{\beta}$ results from viewing earthquake recurrence time in connection with the slip budget. This makes a link between earthquake statistics (the G-R law) and physics (fault characteristics). Specifically, the relationship enables us to explain different ranges of b-values at megathrust faults, in dependence on interplate asperity and coupling distributions, as well as on amounts of sediments and fluids in subduction channels. The approach differs from common interpretations of the G-R law in that the b-value becomes a field variable, not a constant. It is always the Gibbs distribution for a given magnitude range that we use due to our ignorance about the system outcome, and it is the b-value that variates, depending on our knowledge about the system physics. This is important for seismic forecasts, which are mostly based on the G-R relationship.

Key Words: Gutenberg-Richter law, Subduction zone processes, Megathrust earthquakes

1 Introduction

Understanding earthquakes is like solving a jigsaw puzzle: Various pieces, like observations, concepts, and models, are to be collected and fitted together to form a consistent view. The largest, megathrust earthquakes can be viewed from two different angles, referring to their physics (seismic and aseismic slips and the slip budget, asperities and the plate interface heterogeneity, the plate coupling) or statistics (the Gutenberg-Richter (G-R) law and its b-value). However, only after joining these apparently different approaches, a coherent picture of the phenomena can be revealed, possibly leading to more effective earthquake forecasting.

In this paper, several earthquake related concepts are outlined to reveal the G-R law's b-value as the link between earthquake physics and statistics. The physics of megathrust earthquakes is thought of as a process of slip that takes place along the plate interface in a subduction zone; the statistics of earthquakes, or probability of their occurrences, is represented by the earthquake frequency-magnitude relationship. Different b-values can be explained in terms of the slip patterns, or characteristics of the underlying asperity distributions and heterogeneous plate coupling. As an example, high b-value observed in the case of the largest earthquakes is discussed in the present paper.

Finite-fault rupture models are available for the largest earthquakes ($m_W 7.5$ and above) since 1990s [1]. Such models represent earthquake rupture histories described in terms of coseismic slip distributions. They can be used to study the relation between the b-value and the exponent β in the rupture area vs. slip scaling, which has been proposed in the previous paper [2].

2 Theory

2.1 Tectonic loading

In subduction zones, the relative movement of two tectonic plates drives slip movements at their interface, or the megathrust fault. In the long-term, the plate convergence rate, V_P, should be balanced by the same average speed of the slip, V, at each location along the plate interface. The slip deficit rate is defined as the speed difference,

$$\Delta V = V_P - V \ . \tag{1}$$

Thus, the tectonic loading dictates the interface capacity to slip, which grows with increasing slip deficit for $\Delta V > 0$.

2.2 Slip budget

The slip budget of the plate interface includes tectonic loading, or slip deficit accumulation, and its release by slips. At any point, the long-term slip is controlled by the plate convergence rate [3, 4]. The slip deficit is released by seismic and aseismic slip. If the plate interface is locked and cannot keep up with the plate convergence rate, V_P, the plates are deformed and strain energy is accumulated. The deformation is accommodated and strain energy released by slips. The slip deficit, $\Delta V \cdot T$ is accumulated over a period of time, T, in a given region, if the slip rate is lower than the convergence rate, $\Delta V < 0$. The slip deficit should be compensated in the long-term by slips, $\Delta V = 0$.

2.3 Asperities

Slips at a given fault are not uniform, either in space or in time. Asperity models assume that the fault plane consists of strong patches of episodic, unstable slips, which are surrounded by weaker, creeping regions [5]. Slow slips in the non-asperity regions concentrate stresses in the asperity regions during interseismic periods. Asperities accumulate stresses until they break during earthquakes. The stressed regions can be identified by seismic tomography as seismic wave velocity anomalies.

2.4 Coupling

The interplate coupling is defined as the ratio of the slip deficit rate over the plate convergence rate [6]. Regions of high interseismic coupling roughly correspond with high coseismic slip regions in most cases, although the slip deficit release by slow slip events or silent earthquakes can disturb this view. The estimated maximum slip deficit and maximum slip area define the potential for the largest earthquake in a given location [7]. The asperity model approach suggests that the maximum slip or the maximum slip deficit on the fault, i.e., the place on the interface that remains locked for the longest time, can control the potential for possible earthquake magnitude. A coupling coefficient,

$$C = \Delta V / V_P \tag{2}$$

is a measure of coupling between the plates. If $C = 0$ ($\Delta V = 0$), the fault is creeping at its long-term rate. If $C = 1$ ($V = 0$), the fault is fully locked. Coseismic slip is correlated with the interseismic plate coupling.

2.5 Hierarchical asperities

Asperities are not fully coupled: They undergo aseismic slip in the interseismic period. This suggests, that the asperities have internal structures [6]. Aseismic slip within an asperity concentrates stress at internal smaller asperities due to a local difference of slip deficit and enables the occurrence of a smaller earthquake in a rupture area of an asperity. Therefore, the slip rate at a small asperity located within a larger asperity, in the period between the earthquakes rupturing the larger asperity, becomes smaller than in the case that the small asperity is not located within a larger asperity, or after the whole large asperity breaks. The slip rates of these small asperities correspond to the coupling coefficient. The area with a relatively sparse density of large asperities has a higher aseismic slip rate (lower coupling), and the area where the large asperity is located has a relatively high density of asperities and a smaller aseismic slip rate (higher coupling). The largest earthquakes occur when the last, strongest asperity breaks, so the whole large asperity can slip. If such an area remains locked for a time period, T, the accumulated slip deficit, or the maximum possible slip, is

$$D_{MAX} = V_P T \; . \tag{3}$$

The observed maximum and average (over the rupture area) coseismic slips of such earthquakes are smaller than D_{MAX} estimations [1].

2.6 Gutenberg-Richter law

The G-R law relates the earthquake magnitude, m, with the number of events, N, per unit of time in a given region with magnitude m and above. This empirical relation can be written as $\log N(m) = a - b(m - m_T)$, where a and b are constants, m_T is the threshold magnitude. Parameter $a > 0$ depends on the number of all earthquakes with magnitudes m_T or above; parameter $b > 0$ describes proportion of small and large earthquakes. Most earthquake populations exhibit $b \approx 1$. Variations ($0.5 < b < 1.5$) are observed locally, for specific fault patches and for given time periods.

The G-R relationship can be expressed as a probability density function [2]. For an earthquake catalog with minimum magnitude m_T, frequency of occurrences of events with magnitudes m and above, is $F(m) = N(m)/N(m_T) = 10^{-b(m-m_T)}$ ($N(m_T)$ is the total number of earthquakes in the catalog). For the relative magnitude, $u = m - m_T$, the proportion $F(u)$, treated as a cumulative distribution, can be expressed by the density function, $f(u)$, $F(u) = \int_u^\infty f(u')du'$, with

$$f(u) = b'e^{-b'u} \ , \tag{4}$$

with the normalization condition $\int_0^\infty f(u)du = 1$. Here $b' = b \ln 10$ can be estimated by using the magnitude mean value,

$$\int_0^\infty uf(u)du = 1/b' = ln10/b \ . \tag{5}$$

Distributions of this form, known as Gibbs distributions, arise when the system is constraint to have fixed mean value, $< u >$, and maximum information entropy, $I = -\int f(u) \ln f(u)du$, among such fixed mean value systems. The information entropy is a measure of uniformity of distribution $f(u)$, so the Gibbs distribution is the most uniform one given the constraint.

2.7 Earthquake forecasting

Earthquake forecasts can be understood as a probability density functions (pdf) for occurrence of an earthquake with a given magnitude, in a given region and time period. The probability distributions express our knowledge about a given process outcome. The larger our ignorance, the more uniform probability distribution is assigned. Honest forecasts use all and only available information about the seismic system.

The G-R pdf can be obtained as the most uniform distribution for the magnitude, m, under the constrain that the magnitude mean value is fixed.

2.8 MEP approach

In general, the Maximum Entropy Principle (MEP) enables us to find the pdf that is as uniform as possible while agreeing with given constraints suggested by all available information (Jaynes, 2007). To this end, the information entropy, which is a measure of distribution uniformity, is maximized under two constraints, the normalization condition and the mean value.

The G-R relationship, perceived as the Gibbs distribution with the b-value in its exponent, results from the Maximum Entropy Principle under two assumptions: (1) the mean magnitude is assumed as the constraint, and (2) magnitude, so logarithm of seismic moment, is used as an earthquake size measure [2].

For the first point, the constraint is related to the recurrence time, which is implied by the slip budget. To compare two recurrence time estimations, resulting from the G-R relationship and from the slip budget, respectively, the rupture area vs. slip scaling is assumed. This enables us to relate the b-value with asperity fault models or subduction channel processes, as they determine how far a given rupture can propagate, given the accumulated slip deficit of the broken asperity.

For the second point, the answer invokes probability theory and the stochastic view on an earthquake generation processes. Originally, the logarithmic energy scale was proposed to collapse a big range of numbers into a much smaller range. Application of the information entropy requires that the prior density function is chosen. Moment magnitude, or seismic moment logarithm, is uniformly distributed in the case of no constraints or our complete ignorance about the system outcome, so it represents the proper choice.

Note that the stochastic aspect of seismicity is involved in both points. Note also more general meaning of the G-R relationship as the frequency- moment magnitude relation: It is represented by the Gibbs distribution, but the b-value in its exponent variates according to the constraint that is proper for a given earthquake set. Thus, the b-value becomes a field variable. It is always the Gibbs distribution that we use due to our ignorance about the system outcome, and it is the b-value that variates, depending on our knowledge about the system physics or evidence from observations.

2.9 Recurrence time

The recurrence time of earthquakes with magnitudes m or above, T_R, can be defined in two ways, by referring to earthquake statistics and physics, respectively.

In the first case, the G-R relationship is used. T_R is defined as ΔT divided by $N(m)$, i.e., by the number of all earthquakes with magnitudes m or above that occur during the time period ΔT:

$$T_R = \Delta T / 10^{a-b(m-m_T)} \ . \tag{6}$$

Assuming that magnitudes are related to slips, $m_W(D)$, for different slips, D' and D, and $\Delta m_W = m_W(D') - m_W(D)$, we have

$$b\Delta m_W = \log \frac{T_R(D')}{T_R(D)} \ . \tag{7}$$

In the second case, the slip budget is used. An earthquake with its maximum slip, D_{MAX}, requires accumulation of the slip deficit of at least the same value, $D = D_{MAX}$. For the plate convergence rate, V_P, the needed recurrence time is, from eq.(3), $T_R = D/V_P$. Consequently,

$$T_R(D')/T_R(D) = D'/D \ . \tag{8}$$

Thus, the G-R law and the slip budget give

$$b\Delta m_W = \log \frac{D'}{D} \ . \tag{9}$$

2.10 Asperities and b-value

To express the magnitude difference, Δm_W, in terms of slips, D, the rupture area vs. slip scaling is assumed,

$$\log A = \alpha + \beta \log D \ , \tag{10}$$

where α and β are constants. Then, the seismic moment is $M_0 = 10^{\alpha} \mu D^{1-\beta}$, and the moment magnitude, $m_W = C + \frac{2}{3}(1+\beta)\log D$, with $C = (2/3)(\alpha + \log \mu - 9.05)$. The magnitude difference is $\Delta m_W = \frac{2}{3}(1+\beta)\log(D'/D)$. So we have the relation between two different parameters, b and β [2],

$$b = \frac{3}{2(1+\beta)} \ . \tag{11}$$

Parameter b defines proportion of small and large earthquakes. Parameter β defines rupture range, given the accumulated slip deficit at the broken asperity. The former belongs to earthquake statistics, the latter belongs to fault characteristics, or earthquake physics. Thus, these two different views are fitted: We can relate observed b-values with rupture dynamics and its underlying fault characteristics.

Equation (11) enables us to explain observed or expected b-values in terms of the asperity fault models. Assuming $\beta > 0$ (so A increases with increasing D), $b \in < 0, 1.5 >$ according to eq.(11).

Consider then two extreme cases of β values. First, $\beta \to 0$ ($b \to 1.5$) means that the rupture area, A, size does not depend on the slip value, D; consequently, the rupture area size is not correlated with the slip deficit that has been accumulated. Second, $\beta \to \infty$ ($b \to 0$) means that A increases very fast with increasing D, so slips due to broken asperities propagate easily along a given fault. The larger is the accumulated slip deficit, the farther rupture propagates. For $b \approx 1$, the rupture area grows as $D^{0.5}$ [2].

2.11 Slip velocities

Rupture dynamics can be formulated in terms of the evolution equation for slip velocities. The following expression can be used [9]:

$$\frac{\mu}{2v_S}\dot{q}(t,r) = -\Delta s = s^T + s^I[q] - s^F[q] \ . \tag{12}$$

Equation (12) represents the instantaneous radiation of a plane wave from the fault when the shear stress is released. The sum $s = s^T + s^I$ is called the driving stress, with the tectonic loading and interaction terms, s^T and s^I, respectively. The cohesive and frictional stresses are denoted by the term s^F. The last two terms are written as functionals of q. The net stress, $-\Delta s$, is the difference between the driving and cohesive and frictional stresses. The net stress determines the slip velocity.

Consider the uniform slip q on the $L \times L$ square fault patch. In this case, the back stress due to the elastic medium response, which resists the slip movement, represents the interaction stress, s^I; it depends on the slipping area size. The driving stress is

$$s = s^T - k_R q \ , \tag{13}$$

where s_T is assumed constant. The driving stress decrease with increasing slip, due to the back stress, is represented by the interaction stress term, $s^I = -k_R q$, where the stiffness, k_R is [9]

$$k_R = (\mu/4\pi)[(2-\nu)/(1-\nu)](\sqrt{2}/L) \ . \tag{14}$$

The back stress $\approx 8q/L$ for $\mu = 3 \times 10^4$ MPa and the Poissons ratio, $\nu = 0.25$ (L in kilometers, q in meters).

Assume that the cohesive stress is

$$s_F = s_P - k_C q \ , \tag{15}$$

until its residual stress level, $s_F = 0$, is attained at the slip weakening distance, $q = d_C$. The slip movement starts when the tectonic stress attains the cohesive stress peak value, or strength, $s_T = s_P$. The critical stiffness, k_C, is proportional to the rate of the cohesive shear stress decrease,

$$k_C = s_P/d_C \ . \tag{16}$$

Both parameters, s_P and d_C, represent material fault characteristics. The strength can be related to the normal stress.

Figures 1 and 2 illustrate the stress vs. slip dependence given on the right hand side of eq.(12). The cohesive stress lines for two different d_C and s_P values follow eq.(15), with the critical stiffness, k_C, given by eq.(16). The system stiffness lines follow the back stress dependence on the slip, $s_I = -k_R q$, which occurs in eq.(13), for two different L values, as given by eq.(14). The distance between the constant tectonic stress line, $s_T = s_P$, and the line defined by the sum of the cohesive and back stresses, is the net stress proportional to the slip velocity, with its maximum values indicated by arrows.

2.12 Stable and unstable slips

The unstable slip movements start when the driving stress decreases slower than friction during sliding. The driving stress decreases with slip, q, as kq, where k is the system stiffness. The stable to unstable slip transition occurs after the system stiffness exceeds its critical value, $k < k_C$. The stiffness k depends on distribution of slips, or the area of possible slip (it is easier to move larger rupture area), whereas the critical stiffness is related to the plate coupling or cohesive stress dependence on slip displacement (it increases with the increasing slope of the stress vs. slip weakening distance line). The critical stiffness can be exceeded in two ways: (1) by decrease of the system stiffness k (dynamical factor), or (2) by increase of the critical stiffness (material or structural factor).

In the case of the uniform slip on the square fault patch, the system stiffness is $k = k_R$. The unstable rupture occurs if $k_R < k_C$. The slip can continue until $s > s_F$, so it stops at $q_S = s_P/k_R$

The unstable rupture condition, $k_R < k_C$, can be written as

$$L > (\mu/4\pi)[(2-\nu)/(1-\nu)](\sqrt{2}(d_C/s_P) \ . \tag{17}$$

Thus, for given strength, s_P, larger d_C requires larger slipping area size for an unstable rupture.

In general, stable or unstable slip movements depend on distribution of slips and on the concurrently slipping area size, as well as frictional or cohesive stress local characteristics.

Figures 1 and 2 illustrate the stable vs. unstable slip conditions. For the same strength, $s_P = 3.6$ MPa (Fig. 1), two cases of large and small critical stiffness values, respectively $k_C = s_P/d_C = 7.2$ MPa/m and 1.8 MPa/m ($d_C = 0.5$ m and 2 m) are considered. Also two cases of the system stiffness due to the medium back stress response, respectively $k_R = 1$ MPa/m and $k_R = 2$ MPa/m are considered. For the larger patch, $L = 8$ km, $k_R < k_C$ in both cases of large and small critical stiffness, k_C. The maxima 2 and 4 of the net stress are located below the tectonic stress line, so unstable slip movements (i.e., slips under the fixed tectonic stress) are possible. For the smaller patch, however, $L = 4$ km, $k_R < k_C$ only in the case of larger $k_C = 7.2$ MPa/m ($d_C = 0.5$ m), so that the net stress is positive with its maximum value at point 1. For the larger slip weakening distance, $d_C = 2$ m, $k_R > k_C$, and the net stress is negative with its minimum value at point 3 above the tectonic stress line. Only stable slip movements (i.e., slips under increasing tectonic stress) are possible in this case. For larger strength, $s_P = 5.4$ MPa (Fig. 2), in all cases of the critical stiffness, k_C and the system stiffness, k_R, $k_R < k_C$, and the net stress remains positive, so the unstable slip movements are possible. This shows how stable and unstable slip movements depend on material and dynamical system characteristics decide about.

3 Data analysis and discussion

3.1 Large earthquakes

The frequency-magnitude relationship and rupture area scaling obtained for global large ($m_W > 8$) subduction interface earthquakes suggest that (a) their b-value ($b \approx 1.5$) is higher than the value obtained for the global set of smaller events ($b \approx 1$), and (b) rupture area is less well correlated with magnitude for those earthquakes [10].

Figures 3 and 4 illustrate the frequency-magnitude relationships. In the first case (Fig. 3), the finite-fault rupture models database for 36 shallow and intermediate-depth, interface, intraslab subduction zone earthquakes since 1990 is used [10, 1]. Its visual examination suggests $b \approx 1.5$, and eq.(5) gives $b = 1.53$. In the second case (Fig.4), the USGS catalog is used, and the b-value is calculated for 55 global earthquakes since 1950. Equation (5) gives $b = 1.49$; for those data, but the visual estimation of the b-value seems more problematic. Thus, the finite-fault rupture models enable us to get some new insight into earthquake statistics and scaling relations.

According to eq.(11), the b-value close to 1.5 means that β is close to zero, so the rupture area, A, does not depend on the slip value, D, which is consistent with the observed low correlation between rupture area and slip for the largest earthquakes [10]. The finite-fault rupture models database enables us to estimate β in the rupture area vs. slip relation. Figures 5a and b show the log-log plots for the maximum and average slip, respectively. The linear regression lines give negative, close to zero β slopes, with small correlation coefficients, cr, ($\beta = -0.06$, $corr = -0.05$, and $\beta = -0.18$, $corr = -0.13$).

3.2 Asperity model scenarios

For $\beta \approx 0$, the rupture area does not increase with increasing slip deficit. In the case of the largest earthquakes, this result can be explained within the hierarchical asperity model context [6], assuming that such earthquakes occur after the strongest asperity breaks.

The following scenario is suggested by the asperity model. After the broken site slip, the back stress caused by the last locked site in its surrounding is released, so (a) the driving stress increases in the region. Therefore, previously broken smaller asperities can break again, and sites of previous slow or aseismic slip can creep further or speed up. Moreover, (b) since the area of the possible slip becomes larger, the system stiffness in the region drops below the critical value, even if material fault characteristics are fixed and the critical stiffness due to material characteristics, k_C, does not change. Therefore, the aseismic slip can occur at sites of previously aseismic slip [11].

The rupture area of the largest earthquake is related to the area that has not been fully released by previous smaller events due to the back stress from the strongest locked site rather than to the slip deficit accumulated at that site. Therefore, the area size, A, is not correlated with the maximum or average slip, D. The strongest site failure does not contribute to breaking any stronger site, independently on its accumulated slip deficit: It is the last, strongest area within the hierarchical asperity structure. For similar reasons, large b-values are expected at the stable sliding regions, where isolated asperity ruptures are less likely to propagate into the surrounding creeping zones [12].

For smaller earthquakes within the hierarchical asperity structure, increase of the accumulated slip deficit leads to ruptures of stronger and stronger asperities, causing slips over larger and larger areas, so that A is correlated with D. After the largest earthquake occurrence, for a given accumulated slip deficit, D, it is more difficult for the rupture front to propagate among locked asperities because of the lowered tectonic stress: They become isolated islands. Therefore, the scaling exponent β drops, and the b-value increases over the $b \approx 1$ typical value: A increases at lower rate with increasing D [2]. On the other hand, several years or months before the large earthquakes, the strongest locked site increases the driving stresses in its surrounding, causing aseismic slips at weaker places and easier rupture propagation among broken asperities: They become interconnected islands. Therefore, the scaling exponent β increases, and the b-value decreases below the $b \approx 1$ [13, 15, 14]. The b-value increase a few days before the largest earthquake [14], observed in the case of the 2014 Iquique earthquake, can be related to the aseismic slip around the main shock area observed by geodetical methods [16].

4 Discussion and Conclusions

The present paper is an attempt to explain observed earthquake statistics, such as the G-R law's b-value patterns, in terms of earthquake source processes and plate interface characteristics. In particular, this work is focused on the largest megathrust earthquakes and the b-value changes before and after such events. Several related concepts or ideas have been outlined and used for the task: The hierarchical asperity model, the slip budget and earthquake recurrence time, the stable and unstable slip conditions, and the MEP approach to the G-R law.

Two theoretical results are essential for solving the problem. First is relation (11) between the b-value and the exponent β in the rupture area vs. slip scaling [2]. It enables us to relate changing b-value with earthquake rupture dynamics and physical fault characteristics. In this way, the link between earthquake statistics and physics is established. Second is relation (17) between system stiffness and its critical value. It enables us to explain the interplay between seismic and aseismic slips during earthquake cycle.

Explanation of the following observations have been suggested by using these two results in the hierarchical asperity model perspective:

- Large b-value for the largest global earthquakes,
- Decrease of the b-value before the largest earthquake,
- Increase of the b-value after the largest earthquake,
- Increase of b-value increase related to aseismic slip.

In general, the b-value increases when the asperities become more isolated, whereas it decreases when the asperities become more interconected. This conditions change during an earthquake cycle. Some physical processes at the plate interface can be revealed by observing the b-value variations. If some processes leading to the largest earthquakes could be recognized in this way, an effective megathrust earthquakes forecasting would be possible.

Significance of presented results for the earthquake forecasting task and earthquake hazard estimation is also suggested by the MEP approach to the G-R relationship: It is understood as the Gibbs distribution for magnitudes, which represents our ignorance about the seismic system outcome. Our knowledge is limited to the mean value of magnitudes, $< m > \propto 1/b$, and the possible magnitude range, $m \in < 0, m_{MAX} >$. Therefore, the earthquake generation process can be thought of as sampling with constraints, where the constraints are b and m_{MAX} [2]. Honest seismic forecasts and hazard assessments shoud be based on our knowledge about the constraints, and how they change in time, space, and magnitude range.

This work was carried out within statutory activities No. 3841/E-41/S/2018 of the Ministry of Science and Higher Education of Poland.

References

[1] HAYES, G.P., 2017. "The finite, kinematic rupture properties of great-sized earthquakes since 1990", Earth and Planet. Sci. Lett. **468**(2017)94.

[2] SENATORSKI, P., "Effect of slip-area scaling on the earthquake frequency-magnitude relationship", Phys. Earth planet. Int. **267**(2017)41.

[3] HASHIMOTO, C., et al., "The Mw 9.0 northeast Japan earthquake: total rupture of a basement asperity", Geophys. J. Int. **189**,(2012)1.

[4] SCHOLZ, C.H., CAMPOS, J., "The seismic coupling of subduction zones revisited", J. Geophys. Res. **117**(2012)B05310, doi:10.1029/2011JB009003.

[5] LAY, T., et al., "The asperity model and the nature of large subduction zone earthquake occurrence", Earthquake Prediction Research **1**(1982)3–71.

[6] UCHIDA, N., MATSUZAWA, T., "Coupling coefficient, hierarchical structure, and earthquake cycle for the source area of the 2011 off the Pacific coast of Tohoku earthquake inferred from small repeating earthquake data", Earth Planets Space **63**(2011)675.

[7] MORENO, M., et al., "2010 Maule earthquake slip correlates with pre-seismic locking of Andean subduction zone", Nature **467**(2010)198.

[8] JAYNES, E.T., Probability Theory: The Logic of Science (edited by G. Larry Bretthorst), Cambridge Univ. Press (2007).

[9] SENATORSKI, P., "Slip-weakening and interactive dynamics of an heterogeneous seismic source", Tectonophysics **344**(2002)37.

[10] ALLEN, T.I., HAYES, G.P., "Alternative rupture-scaling relationships for subduc-tion interface and other offshore environments", Bull. Seismol. Soc. Am. **107**(2017)1240.

[11] JOHNSON, K.M., et al., "Challenging the rate-state asperity model: Afterslip following the 2011 M9 Tohoku-oki, Japan, earthquake", Geophys. Res. Lett. **39**(2012)L20302, doi:10.1029/2012GL052901.

[12] VOROBIEVA, I., et al., "Break of slope in earthquake size distribution and creep rate along the San Andreas Fault system", Geophys. Res. Lett. **43**(2016)6869, doi:10.1002/2016GL069636.

[13] NANJO, K. Z., et al., "Decade-scale decrease in b value prior to the M9-class 2011 Tohoku and 2004 Sumatra quakes", Geophys. Res. Lett. **39**(2012)L20304.

[14] SCHURR, B.,et al., 2014. "Gradual unlocking of plate boundary controlled initiation of the 2014 Iquique earthquake", Nature **512**299.

[15] PAPADOPOULOS, G. A., MINADAKIS, G., "Foreshock Patterns Preceding Great Earthquakes in the Subduction Zone of Chile", Pure Appl. Geophys. **173**(2016)3247.

[16] SOQUET, A., et al, "An 8 month slow slip event triggers progressive nucleation of the 2014 Chile megathrust", Geophys. Res. Lett. **44**(2017)doi:10.1002/2017GL073023.

Figures and Tables

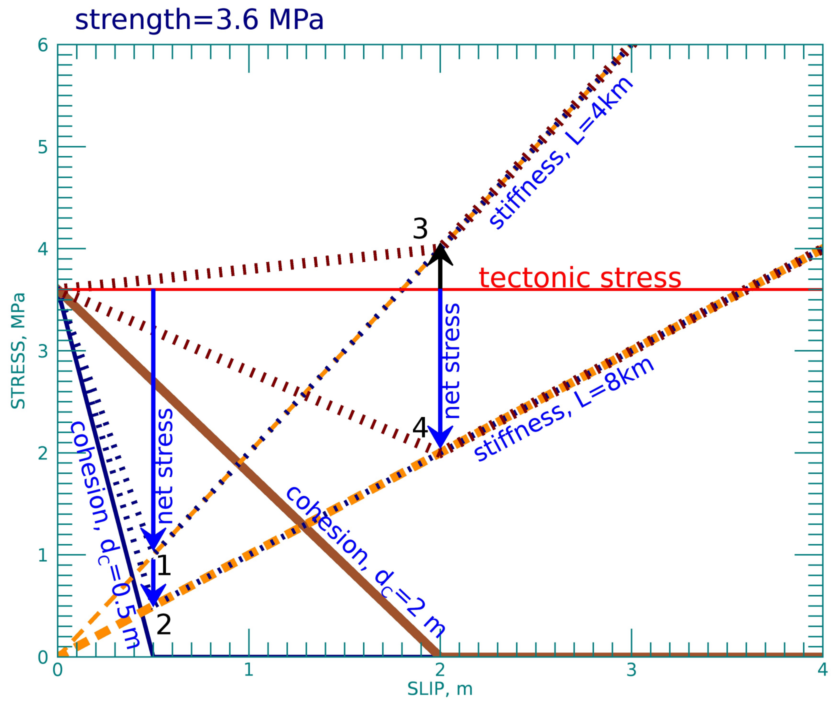

Figure 1: Illustration of a slip-dependent friction law and its stability regimes. Stresses as functions of slip are shown: (1) cohesive stress for two different slip weakening distance values, $d_C = 0.5$ m and $d_C = 2$ m, and the same peak stress values, $s_P = 3.6$ MPa are (solid lines, respectively); back stress for the case of uniform slip along a square patch $L \times L\ km^2$, for two stiffness values, $k_R = 1(L = 8\text{km})$ and $k_R = 2$ MPa/m ($L = 4$km) (dashed lines); resisting stress in four cases (cohesive plus back stress (dotted lines); fixed tectonic stress (horizontal line). The residual friction stress is zero. Vertical arrows show maximum net stresses (labels 1-4). The arrow directed upwards represent the stable slip case ($k_R < k_C$, Table 1).

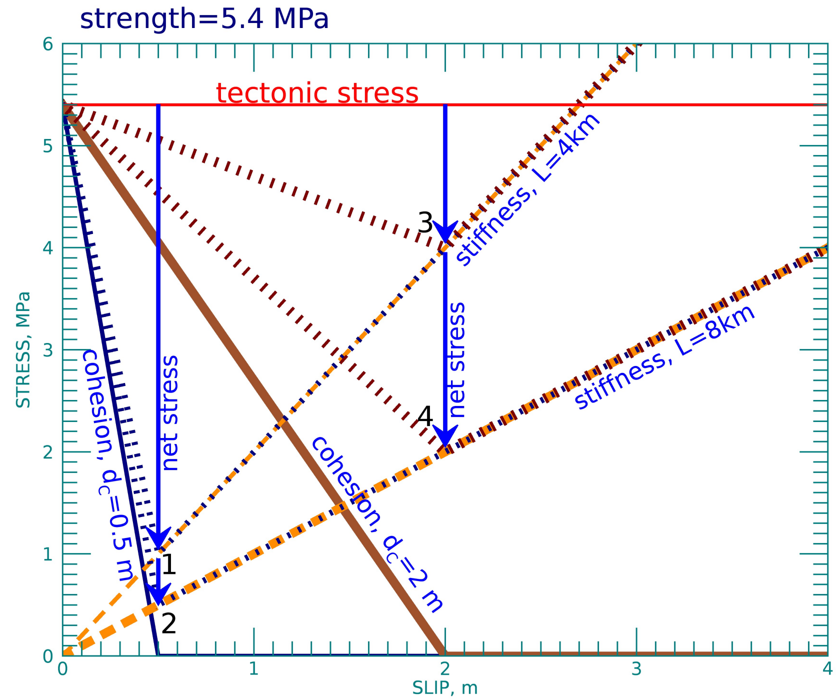

Figure 2: Same as in Fig.1, for $s_P = 5.4$

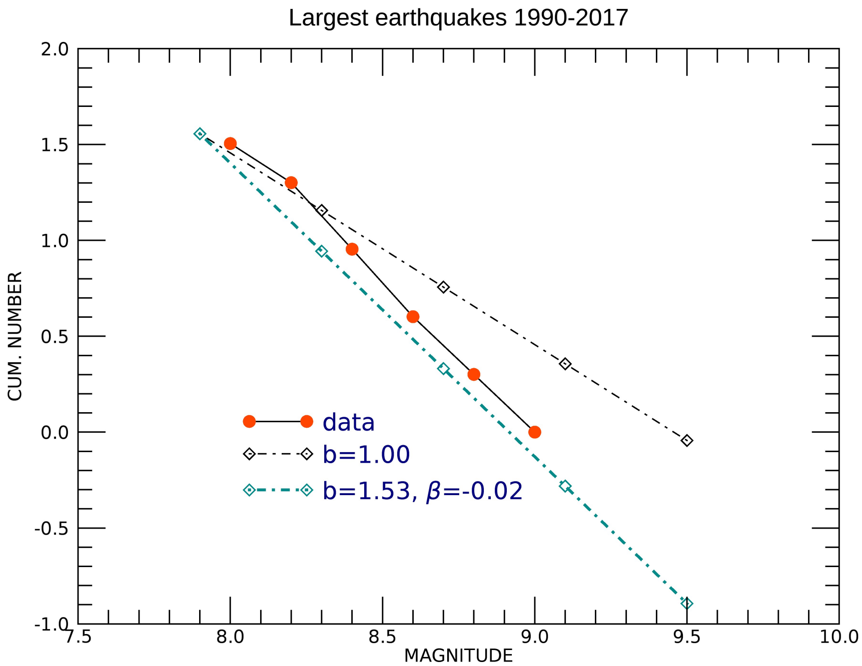

Figure 3: Cumulative magnitude-frequency distribution of global large earthquakes, $m_W > 8.0$, since 1990. The finite-fault rupture models database is used [10, 3]. The b-value is calculated from eq.(5), β-value - from eq.(11)

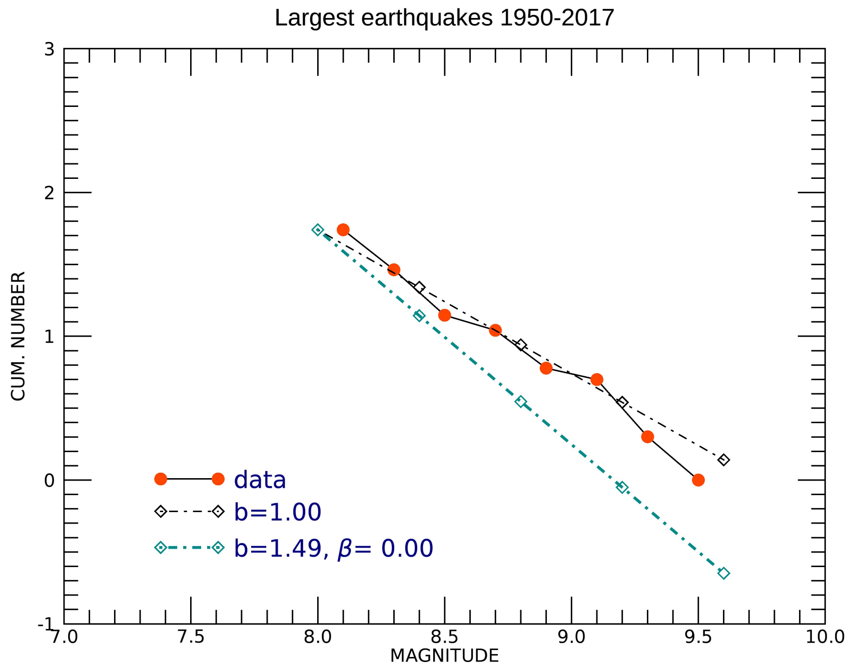

Figure 4: Same as in Fig.3 for global large earthquakes since 1950. The USGS catalog is used.

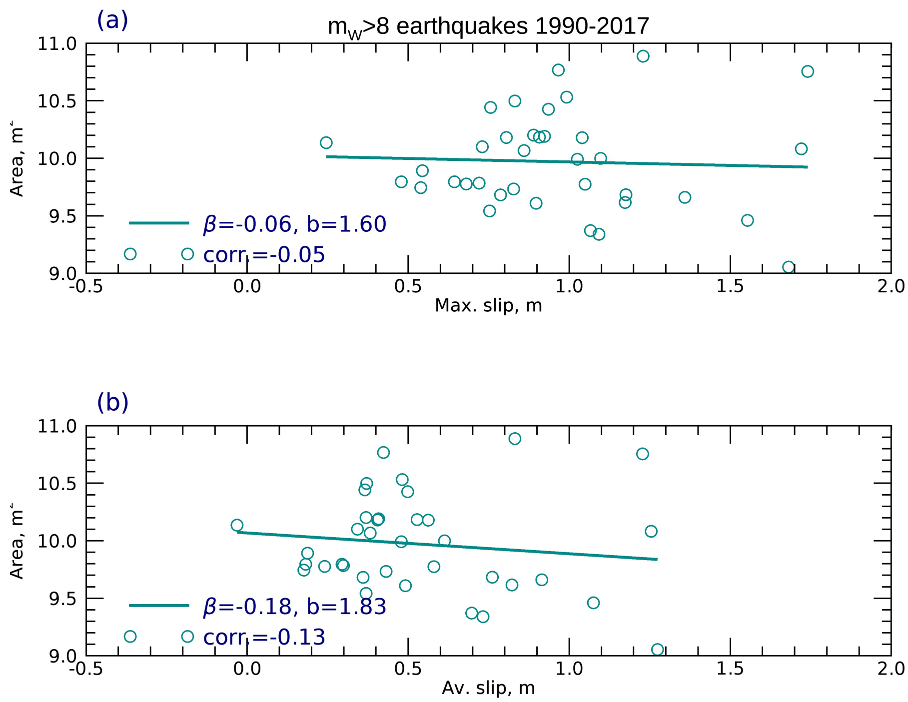

Figure 5: Area vs. maximum slip (a) and area vs. average slip (b) relationships for global large earthquakes, $m_W > 8.0$, since 1990. The finite-fault rupture models database is used [10, 3]. The β-value is calculated by linear regression, and the correlation coefficient is given. The b-value is calculated from eq.(11).

Table 1: Model parameters used in Figs.1 and 2. For two s_P values in Figs.1 and 2, four cases of the d_C and L values are labelled as 1-4 in each of the figure. Values of k_C and k_R, and the stability conditions are shown in three left columns.

Fig.-label	s_P, MPa	d_C, m	L, km	k_C, MPa/m	k_R, MPa/m	stability
Fig.1-1	3.6	0.5	4.0	7.2	2.0	unstable
Fig.1-2	3.6	0.5	8.0	7.2	1.0	unstable
Fig.1-3	3.6	2.0	4.0	1.8	2.0	stable
Fig.1-4	3.6	2.0	8.0	1.8	1.0	unstable
Fig.2-1	5.4	0.5	4.0	10.8	2.0	unstable
Fig.2-2	5.4	0.5	8.0	10.8	1.0	unstable
Fig.2-3	5.4	2.0	4.0	2.7	2.0	unstable
Fig.2-4	5.4	2.0	8.0	2.7	1.0	unstable